Microsc. Microanal. 11, 1–8, 2005
DOI: 10.1017/S1431927605050609

Microscopy AND Microanalysis

Measuring Surface Topography with Scanning Electron Microscopy. I. EZEImage: A Program to Obtain 3D Surface Data

Ezequiel Ponz,[1] Juan Luis Ladaga,[2] and Rita Dominga Bonetto[1]*

[1] *Centro de Investigación y Desarrollo en Ciencias Aplicadas Dr. Jorge J. Ronco (CINDECA) CONICET—UNLP, 47 No. 257-CC 59, 1900 La Plata, Argentina*

[2] *Facultad de Ingeniería de la Universidad Nacional de Buenos Aires, Departamento de Física—Laboratorio de Láser, Paseo Colón 850, Ciudad Autónoma de Buenos Aires, Argentina*

Abstract: Scanning electron microscopy (SEM) is widely used in the science of materials and different parameters were developed to characterize the surface roughness. In a previous work, we studied the surface topography with fractal dimension at low scale and two parameters at high scale by using the variogram, that is, variance vs. step log–log graph, of a SEM image. Those studies were carried out with the FERImage program, previously developed by us. To verify the previously accepted hypothesis by working with only an image, it is indispensable to have reliable three-dimensional (3D) surface data. In this work, a new program (EZEImage) to characterize 3D surface topography in SEM has been developed. It uses fast cross correlation and dynamic programming to obtain reliable dense height maps in a few seconds which can be displayed as an image where each gray level represents a height value. This image can be used for the FERImage program or any other software to obtain surface topography characteristics. EZEImage also generates anaglyph images as well as characterizes 3D surface topography by means of a parameter set to describe amplitude properties and three functional indices for characterizing bearing and fluid properties.

Key words: dense height map, dynamic programming, fast cross correlation, program, 3D surface topography in SEM

Introduction

Scanning electron microscopy (SEM) is very versatile and is largely used for material characterization because of its high lateral resolution and large depth-of-field. Particularly, we studied different parameters to characterize the texture of periodic or quasiperiodic images, for example, the fractal dimension D at low scale, a parameter to characterize the periodic region d_{per} at high scale, and the crossover between the fractal and the periodic regions d_{min} (Bonetto & Ladaga, 1998; Bonetto et al., 2002; Ladaga & Bonetto, 2002). The FERImage program (available free of charge) was developed to obtain these three parameters with the variogram method as well as the fractal dimension with the Fourier method (Bianchi & Bonetto, 2001). The anisotropic samples can be studied by means of the topothesy by using the intercept and the slope of the variogram straight line or the power spectra Fourier straight line (cf., Sayles & Thomas, 1978; Russ, 1994; Thomas et al., 1999 and references therein; Bonetto et al., 2002). As it is known, the changes in gray levels in an SEM image are not directly related to changes in height data but rather to changes in slope (although this last affirmation is only partially true because, according to the samples, the image brightness can be affected by the enhanced emission from edges and ridges, and effects of surface contamination such as local oxidation, not to mention gross compositional variations, also influence brightness). These facts limit the attainment of surface roughness parameters and their comparison with those obtained using other methods, such as a 2D stylus profiling device or atomic force microscopy, among others. In the SEM, a stereo pair, that is, two images of the same area obtained from two different tilt angles to provide separate points of view, allows us to obtain these height data. The first stage for obtaining height data is to find the corresponding disparity (parallax) data between the two images of the stereo pair. The main problem of this technique lies in the difficulty in obtaining quickly reliable disparity values for a whole image, that is, the matching of points in both images. Sun (2002) implemented a method which uses fast cross correlation, rectangular subregioning (RSR), and a new two-stage dynamic programming (TSDP) technique in a

Received November 8, 2004; accepted May 23, 2005.
**Corresponding author*. E-mail: bonetto@quimica.unlp.edu.ar

coarse-to-fine scheme to produce a dense disparity map. His algorithm, tested on several different synthetic and optic real images, showed to be fast and reliable.

In this work, we developed the program, EZEImage, by using fast cross correlation and TSDP to obtain dense height maps from SEM images. In a first stage we must obtain the dense disparity map. In the method implementation to obtain these disparities, we had to use our own strategy to solve specific problems resulting from the different stages that were not explained in Sun's paper, for example, to solve the indetermination in the correlation coefficients when the same gray color in the image in a large area exists and the variances corresponding to left and right SEM images take the zero value. The case of SEM images is different from the one of optic images: fundamentally because for a small homogeneous region of the sample, the same gray level in the SEM images is related to the same surface slope, whereas the same gray level on optic images is related with the same surface height. In the case of the stereo pair of SEM images, the height data are proportional to these disparity values only if working with zero initial tilt angle, and the stereo pair is obtained by tilting the sample $a \pm \Delta\phi$ angle from this position. To work with any initial tilt angle and any rough sample, a suitable function for the height calculation from these disparities must be used. In addition, a strategy should be chosen to avoid the problems of the magnification and working-distance variations when the sample is tilted. These problems are avoided in our program by imposing that the image center coincides with the eucentric point and by taking it as a reference point to obtain all the heights referred to this. The eucentric has zero disparity value at any tilt of the sample and it belongs to the tilt axis since the eucentric is the point where the tilt axis intercepts the optic axis. Taking the eucentric as image center is an advantage in maintaining the perpendicular lines at tilt axis (epipolar lines) on both images, that is, the disparities of points belonging to a certain epipolar line on the left image are measured in the same epipolar line on the right image, which is a demand to use Sun's algorithm. Another advantage of the coincidence between the eucentric and the image center is that the equation used for height calculations produces fewer errors since the number of required measurements is lower than in the case where the previous condition is not fulfilled.

There are several commercially-available software packages that generate height maps for SEM images, but not all of them work at any initial tilt angle and, as far as we know, EZEImage is the only one that has the advantage of a TSDP technique. Using this technique will have the effect of filling the holes where undefined coefficient-correlation values exist in areas with little texture in the image, provided these areas are not too large.

Although the principal objective of our software is to obtain reliable 3D data of SEM images, the program also allows us to obtain anaglyph images, dense disparity maps, and area bearing ratio. The obtained height image (dense height map) can be used with the program, FERImage, to obtain, among other things, the fractal dimension by the variogram and Fourier methods. Both programs are well complemented because in many cases, only an SEM image allows us to quickly characterize a sample through the d_{per}, d_{min}, and D parameters and also to study anisotropic samples with the topothesy. The quantitative stereo microscopy involves some extra effort to obtain stereo pairs in a correct way, but the information obtained with the height values is invaluable and, in these cases, the EZEImage program will play an important role.

The program also allows us to choose any size area of the height image and to obtain the necessary data to calculate fractal dimension from the variogram and from the log–log graph of area versus step. A data set to obtain the area bearing ratio curve is also available. In addition, it is possible to obtain a parameter set for characterizing amplitude and three functional indices for characterizing bearing and fluid-retention properties as suggested by Dong et al. (1994). These indices were introduced in the program because, as it was considered by their authors, they are more meaningful and more universal than other functional parameters in characterizing different kinds of surfaces.

Fast Stereo Matching Algorithm

The algorithm is based on Sun's work (2002) that uses four constraints to obtain the correct match: (1) it works on epipolar rectified stereo images so the matching points lie on the same image scanlines of the stereo pair. This means that in the present program the tilt axis will be exactly vertical and the image center will be the eucentric point. (2) Matching should be unique between the two images. (3) Local regions of the disparity map should be relatively smooth. (4) The points along the corresponding epipolar lines in both images of the stereo pair have to occur in the same order.

Since the zero mean normalized cross-correlation coefficient is independent from differences in brightness and contrast, it is used to decide which point on the second image g is the most similar to the chosen point on the original image f:

$$C(i,j,s) = \frac{\mathrm{cov}_{i,j,s}(f,g)}{\sqrt{\mathrm{var}_{i,j}(f)\mathrm{var}_{i,j,s}(g)}}, \tag{1}$$

where

$$\begin{aligned}\mathrm{cov}_{i,j,s}(f,g) &= \sum_{m=i-K}^{m=i+k}\sum_{n=j-L}^{n=j+L}(f_{m,n}-\bar{f}_{i,j})(g_{m,n+s}-\bar{g}_{i,j+s}) \\ &= \sum_{m=i-K}^{m=i+k}\sum_{n=j-L}^{n=j+L} f_{m,n}g_{m,n+s} \\ &\quad -(2K+1)(2L+1)\bar{f}_{i,j}\bar{g}_{i,j+s},\end{aligned} \tag{2}$$

$$\mathrm{var}_{i,j}(f) = \sum_{m=i-K}^{m=i+k} \sum_{n=j-L}^{n=j+L} f_{m,n}^2 - (2K+1)(2L+1)\bar{f}_{i,j}^2 \quad (3)$$

$$\mathrm{var}_{i,j,s}(g) = \sum_{m=i-K}^{m=i+k} \sum_{n=j-L}^{n=j+L} g_{m,n+s} - (2K+1)(2L+1)\bar{g}_{i,j+s}^2, \quad (4)$$

and $f_{i,j}$ is the intensity value of a pixel in the position (i,j) of the $M \times N$ image f; $\bar{f}_{i,j}$ is the mean value within the local correlation window of $K \times L$ size. Similar definitions are given for the second image g; s corresponds to the shift of the window in the second image along epipolar lines and represents the possible disparity values. Hereafter, we will call the original and second images left and right images, respectively. For any point on the left image, the searched disparity, that is, the s value, can be varied from $-d$ to $+d$ on the right image, if d is chosen as an estimated initial value. The whole correlation coefficient number defines a 3D correlation volume of $MN\mathcal{D}$ size, where the maximum disparity search range $\mathcal{D}$ is equal to $(2d+1)$. Fast calculations of local mean, variance, and covariance were achieved by using the box-filtering technique. Similarly, fast cross correlation of two images was calculated by using the same box-filtering idea (Sun, 1998, 2002).

The algorithm implemented here provides optimal solution for obtaining the disparity map from the 3D correlation volume and it is based on the new fast Sun's algorithm. We only use fast cross correlation and the TSDP technique to obtain a maximum-surface from this 3D volume. In the first stage, an accumulated intermediate 3D volume Y in the vertical direction for each vertical slice j is obtained. It contains the accumulated values of the maximum cross-correlation coefficients for each vertical j slice of the same 3D volume. This intermediate volume is created from top to bottom, the top horizontal slice being a copy of the top slice of the correlation coefficient volume:

$$Y(0,j,s) = C(0,j,s). \quad (5)$$

For the other horizontal slices, the Y values at the (i,j) position are obtained as

$$Y(i,j,s) = C(i,j,s) + \max_{k::|k| \le p} Y(i-1, j, s+k). \quad (6)$$

Here, p is the number of local pixels that will be checked. Values of p higher than 1 can be used but the calculation time will be increased. In the second stage of the TSDP algorithm, the bottom horizontal slice of the intermediate volume is selected and by using dynamic programming technique, it finds the shortest path from left to right in this two-dimensional (2D) slice (for more information about the 2D shortest-path extraction using dynamic programming, see Buckley et al., 1997). Then, the next horizontal slice is selected and by masking out pixels, which are further than p pixels from the shortest path obtained from the previous slice, a new shortest path is found. When all the slices have been processed, the disparity map is obtained with all the shortest paths from each of these slices. In this way, the algorithm allows us to obtain a smoother surface by taking all the information into account instead of taking only the information of each individual epipolar line. The subpixel accuracy was implemented by fitting a second-degree curve to three correlation coefficients neighboring the obtained disparity values and by taking the extreme of the curve. More computational speed can be achieved by implementing the RSR for fast similarity measures working in the coarse-to-fine scheme, but it is not implemented in our program version. The algorithm implemented here is restricted to simply-connected surfaces and it does not solve the occlusion problems. Some blurring effects also may occur at depth discontinuity region. As the algorithm works with cross-correlation, some unmatched- or incorrectly-matched points are produced if there are large areas with little texture that would appear in the height map as noise. The use of the TSDP partly allows us to solve the problem when the area is not too big because this technique has the effect of filling the holes produced by undefined correlation coefficients. For more details about the TSDP see Sun (1998, 2002). By using a greater window size, it is possible to obtain better results in big areas with little texture, but in this case, information may be lost on more contrasted regions. In this program version no other filtering technique was used to eliminate that noise because it is not easy to find one technique that does not produce systematically, fractal-dimension values lower than the correct ones, for example, when the hybrid-median filter is used (see Ladaga & Bonetto, 2002).

Dense Height Map

Once the dense disparity map was obtained, the dense height map could be calculated. These height values $z(i,j)$ were measured with respect to a plane that contains the tilt axis and forms an angle of $(90 - \phi_1)$ with the optic axis:

$$z(i,j) = \frac{x_1(x_2 \sin\phi_2/(WM) + \cos\phi_2) - x_2(x_1 \sin\phi_1/(WM) + \cos\phi_1)}{M[(1 + x_1 x_2/(WM)^2)\sin(\phi_2 - \phi_1) + (x_1 - x_2)\cos(\phi_2 - \phi_1)/(WM)]}, \quad (7)$$

where W and M are the working distance and the magnification respectively, ϕ_1 and ϕ_2 are the tilt angles corresponding to the left and right images respectively, x_1 is the pixel position (i,j) whose height value needs to be known on the left image, and x_2 is the pixel position of same point on the right image (measured in the epipolar and by taking the image center as coordinate origin). The x_1 and x_2 parameters are measured in the same units as W. In a previous stage, where x_1 and x_2 are expressed in pixel units, the

Table 1. A Parameter Set to Characterize the Surface Topography of Four Approximately Gaussian Engineered Samples

Sample	S_q (μm)	S_{ke}	S_{ku}	S_z (μm)	S_{bi}	S_{ci}	S_{vi}
Shot blasted	13.088	−0.108	2.996	121.696	0.615	1.524	0.125
FEPA #1000	10.609	0.350	3.921	111.828	0.586	1.639	0.104
FEPA #800	11.844	−0.382	4.470	130.099	0.653	1.419	0.137
FEPA #500	18.654	−0.552	5.161	190.620	0.655	1.422	0.157

x_2 value can be obtained from the disparity value s as $x_2 = x_1 + s$.

Equation (7) is a simplification of the one obtained by Lane (1972), taking into account that the image must be obtained in the eucentric position and with the image center as reference point in our program. In Lane's original equation only the magnifications and working distances for the reference point of left and right images must be known. With the eucentric as reference point in our program, the work distance W and the magnification M are equal on both images. The program allows us to choose other reference points to obtain height values with respect to these points. In the case of our program, it is indispensable that the eucentric point exactly coincides with the image center and that the tilt axis is exactly perpendicular to the axis where the disparities are measured on the image, that is, to the epipolar line. To find the eucentric point, it is convenient to choose a remarkable structure in the sample that occupies the screen center that will be the center of the left image. The eucentric point is correctly chosen if the same pixel of the sample is present in the center of the left and right images. The whole calculation is based on these hypotheses and wrong values will be obtained if this is not fulfilled. It is always better to obtain a good stereo pair according to these conditions; however, if the tilt condition is not fulfilled then the image must be rectified. The image rectified will allow us to obtain better height values but also will present digitization errors and in some cases, and according to the required parameter, it could be better not to rectify the image for a very little tilt shifting.

To estimate the tolerance in the shift of the tilt axis each sample must be particularly analyzed. In the following section, samples of emery papers will be studied and a set of parameters will be calculated and shown in Table 1. By studying this set and also the d_{per}, d_{min}, and D parameters (these last parameters will be fully studied in part II of this work by Bonetto et al., 2005), we found a tolerance of two degrees for the tilt axis shifting for almost all parameters. The observed variations in d_{per}, d_{min}, and D were within the calculation errors. The variation in the three functional parameters was close to 1% in all cases. The other parameters showed different variations according to the sample but they were smaller than 10%, except for the skewness, which was the most affected parameter, and in some cases this overcame this percentage. An error of 5% in the magnification and a lack of precision of one degree in $(\phi_2 - \phi_1)$ were completely imperceptible for all the parameters except for S_q and S_z, however, which showed smaller variations than 10%. These conclusions are valid for both of the optic working distances 22 mm and 44 mm.

At this point, it is important to study the maximum error in the height values obtained here and for this purpose we worked with a simplified equation. For high magnifications, height values in pixel units between any point on the image and the eucentric point can be obtained from the following equation:

$$z = \frac{x_1 \cos(\phi_2 - \phi_1) - x_2}{\sin(\phi_2 - \phi_1)}. \tag{8}$$

Taking into account the disparity $s = x_2 - x_1$, the maximum error (Δz^*) is

$$\Delta z^* = \frac{\Delta x_1(\cos(\phi_2 - \phi_1) + 1) + \Delta s}{\sin(\phi_2 - \phi_1)}. \tag{9}$$

Due to the fact that the images are digitized, we can take for $|\Delta x_1|$ and $|\Delta s|$, in a first approximation, values of 0 and 1 pixel, respectively. With these approximations $\Delta z^* \sim 1/\sin(\phi_2 - \phi_1)$. The precision in the third dimension is an order of magnitude or so worse than the lateral resolution of the images for $(\phi_2 - \phi_1)$ between 1 and 5 deg and there is a smaller relationship than 5 to 1 for $(\phi_2 - \phi_1)$ between 10 and 20 deg. This is because an s disparity value will correspond to all close spatial points that have disparity values between s and $s \pm 1$ in order to be distinguished in image regions with monotonously increasing or decreasing heights. This is due to the fact that the disparity is an integer number on a digital image. A disparity value $s \pm 1$ will correspond to the next value close to the end value of the previous range and the next close values will have the same disparity value $s \pm 1$ until the disparity value changes again ± 1. This fact will show a jump $(\sim 1/\sin(\phi_2 - \phi_1))$ between two different "plateaus" with constant height values. This jump will be higher if the disparity changes in $\pm$ an integer number higher than 1. The subpixel approximation implemented in the program in the epipolar (X axis) allows us to increase the precision in the values of the height differences, reaching an equal or smaller value than the lateral resolution depending on the $(\phi_2 - \phi_1)$ value. But this precision that allows us to obtain a greater information among close points occurs only on the "plateaus." Therefore, this enhancement cannot be interpreted as a greater accuracy on the calculated height values because the existence of the error shown in equation (9) is always present. Although the calculation of the maximum error was obtained with the expression corresponding to high magnification, these conclusions are also valid for low magnification. Effectively, in the images studied in this article, which were obtained at one 100× magnification and with $(\phi_2 - \phi_1) =$ 10 deg, the observed-average jumps were of ~5.6 pixels, which were very near the value of $1/\sin(10) \approx 5.76$ pixels. The subpixel approximation allowed us to observe height differences as small as 0.2 pixels in the "plateaus" in these samples.

Outline of the Program

EZEImage enables us to work with 8-bit images in bitmap format. It provides five options for image analysis.

Anaglyph Image

This alternative generates an anaglyph image in red–blue or red–cyan colors to view stereoscopic images using colored spectacles.

Dense Height Map

This option produces a dense disparity map from a stereo pair of SEM images. From these disparities, a dense height map is obtained as shown previously. If the microscope only allows horizontal tilt axis, the images must be rotated 90 deg counterclockwise before being loaded into the EZEImage program. In this option, five output files are given:

1. *Height File*. This is a text file containing the height values in microns corresponding to the input image.
2. *Disparity Map*. The disparity values are given in bitmap format in gray levels, and the corresponding values in pixels can be obtained by taking into account the maximum and minimum disparity that are displayed in the menu or are written in the text file. This option allows us to study images from other sources provided that their epipolars are horizontal. By using the corresponding expressions, the height values can be obtained.
3. *Height Map*. The height values are given in bitmap format in gray levels, and the corresponding values in microns can be obtained taking into account the maximum and minimum height that are displayed in the menu or are written in the text file. The plane containing the tilt axis is taken as the reference datum for the calculation. The height values are calculated regarding the reference point; that is, its height value is taken as zero. If it is not given, the image center will be taken by default as the reference point. This file can be used with the FERImage program to obtain the d_{per} and d_{min} parameters and also the fractal dimension. Because the FERImage program works only with square images, the option Crop (also available in this program) can be used for this purpose.
4. *Residual Height Map*. Similar to the Height Map but in this case, the least-squares mean plane was taken as the reference datum.
5. *Binary Data File*. This file has all the data calculated in binary format. It is necessary for other options such as Height View, Parameters, and Bearing Area.

Two options are implemented: Whole Image and Valid Region. In the first case, disparity and height values are calculated for a central region of size $(N - 2w) \times (M - 2w)$ for a stereo pair of size $N \times M$ and a local correlation window of $w \times w$ size. But one must bear in mind that the region that has the valid disparity values is a central region of size $(N - 2d - 2w) \times (M - 2w)$ for a stereo pair of $N \times M$ and an estimated initial disparity value d. The second option works with a centered stereo pair of size $(N - d - w) \times (M - w)$. In this case, each pixel on the left image will be correlated with some pixel on the right image. We recommend working in this last mode to avoid using wrong values and to reduce the time of calculation.

In Figure 1a, an SEM image of a silicon sample with an average thickness of 190 μm (value obtained with a micrometer) is shown. This image was obtained with a Philips SEM 505 with a magnification of 200× and an optic working distance of 44 mm. The white frame shows the valid region for the height values. The corresponding dense height map is displayed in Figure 1b and the height values were calculated with the image center as the reference point. The local correlation window size was 4×4 pixels, the searched disparity d was 62 pixels, and the obtained maximum disparity was 61 pixels. The two SEM images of the stereo pair were taken at 40 and 45 deg, respectively. Taking into account that the sample had irregular edges, we can say that reliable values of the silicon thickness in different places with the dense height map were obtained. The observed dispersion in the values was around 10% with respect to the micrometer values.

Another example is shown in Figure 2 corresponding to a surface prepared by shot blasting (Fig. 2a). In this case, the image was obtained with a magnification of 100× and an optic working distance of 22 mm. The white frame shows the valid region for the height values. The local correlation window size was 4×4 pixels, the searched disparity d was 20 pixels, and the obtained maximum disparity was 18 pixels. The corresponding dense height map, calculated with the center of the image as the reference

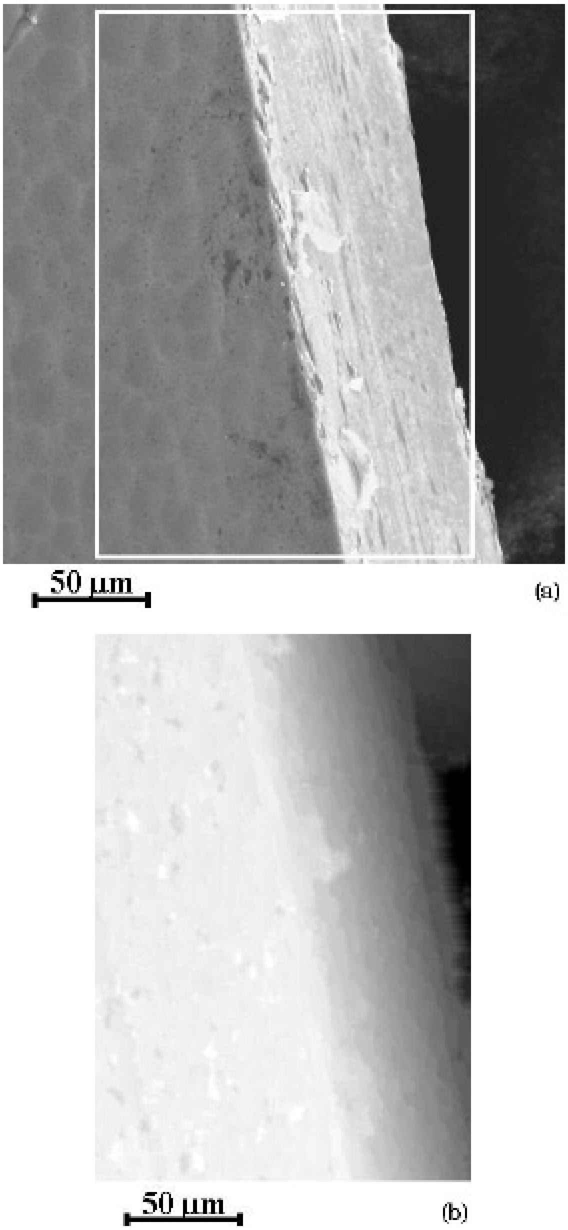

Figure 1. The SEM image with the frame showing (a) the valid region and (b) the dense height map corresponding to SEM images of a silicon film.

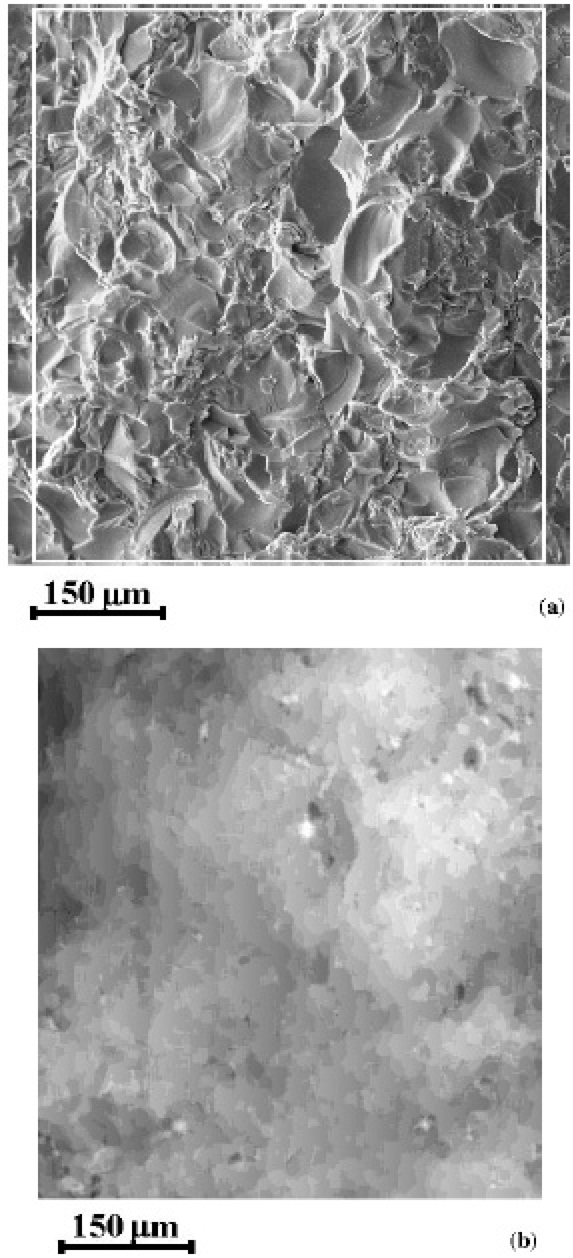

Figure 2. The SEM image with the frame showing (a) the valid region and (b) the dense height map corresponding to SEM images of a shot-blasted surface.

point, is shown in Figure 2b. The two SEM images of the stereo pair were taken at 10 and 20 deg, respectively.

Relative Height

This option calculates the difference of heights between two points from a stereo pair of SEM images and is preferably used when the height information of a few points are required. This option also is used to find values on images with a large area containing little texture where the matching results on the dense height map option could not be valid.

Parameters

This program calculates a parameter set for characterizing amplitude and some functional properties to study the surface topography. The four parameters to describe amplitude properties are: (1) root-mean-square deviation of surface topography S_q; (2) ten-point height of surface topography S_z; (3) skewness of topography height distribution S_{sk}; and (4) kurtosis of topography height distribution S_{ku}. The three functional indices that are based on the analysis of the surface Abbott-Firestone curve characteristics are: (1) surface bearing index S_{bi}; (2) core fluid retention index S_{ci}; and (3) valley fluid retention index S_{vi}. These seven parameters are calculated by using the residual surface, $h(i,j)$, which is the difference between the original surface $z(i,j)$ and the least-squares mean plane $f(i,j)$ taken as the reference datum (see Stout et al., 1993 and Dong et al., 1994 for more details about these topics).

Table 1 shows the values of the parameter set for the surface of three emery paper FEPA #1000, #800, and #500, and for a surface prepared by shot blasting corresponding to a central area of 444×444 pixels ($\sim 560 \times 560$ μm). For the dense height map calculation, in all the cases, the two SEM images of the stereo pair were taken at 10 and 20 deg with an optic working distance of 22 mm and a local correlation window of 4×4 pixels. The values corresponding to a Gaussian surface for the functional indices S_{bi}, S_{ci}, and S_{vi} are 0.608, 1.56, and 0.11, respectively. The values obtained with the EZEImage program agree with the expected range for approximately Gaussian engineered surfaces as shown by Dong et al. (1994) in studies with profiling techniques. In the case of the emery papers, it can be observed that the bigger grain size (smaller # number), the higher the S_q and S_z values. All of these results allow us to state that the EZEImage program provides a reliable dense height map.

In the Parameters option, it also is possible to obtain the area data for different window sizes and the variance data for different step sizes. The fractal dimension can be obtained with a graph of these values in log–log scale. In addition, the necessary data to plot the bearing area curve are also supplied.

View Height

This alternative allows us to view the corresponding heights of each pixel of the loaded image in the current EZEImage window by clicking twice on that pixel. These heights are given regarding the reference point (the image center by default). We used this option with the 190-μm-thick silicon sample shown in Figure 1 and found that the results obtained with the dense height map and the relative heights were equal. The different values from 190 μm that were obtained in different regions of the sample were not $>$10%, but this agrees with the irregular shape of the edge.

Conclusion

A program to study 3D surfaces in SEM was implemented. The use of fast cross correlation and TSDP allows the quick attainment of a reliable dense height map. The EZEImage program will be an important working tool in the surface characterization and, fundamentally, will allow us to take advantage of all of the possibilities of the FERImage program using the dense height map as an input image. The EZEImage program is freely available for research purposes only. If this software is found useful in journal publications or conference presentations, mention this article in the references.

Acknowledgments

This work was supported by Consejo Nacional de Investigaciones Científicas y Técnicas (CONICET) of Argentina. The authors thank Dr. Changming Sun for his comments regarding questions that emerged while reading his paper. The authors thank Dr. Elena Forlerer for supplying the emery papers and Dr. Mario Sánchez and Dr. María Elena Canafoglia for their assistance in the attainment of SEM images.

References

Bianchi, F.D. & Bonetto, R.D. (2001). FERImage: An interactive program for fractal dimension, d_{per} and d_{min} calculation. *Scanning* 23, 193–197.

Bonetto, R.D, Forlerer, E. & Ladaga, J.L. (2002). Texture characterization of digital images which have a periodicity or a quasi-periodicity. *Measure Sci Technol* 13, 1458–1466.

Bonetto, R.D. & Ladaga, J.L. (1998). The variogram method for characterization of SEM images. *Scanning* 20, 457–463.

Bonetto, R.D., Ladaga, J.L. & Ponz, E. (2005). Measuring surface topography by scanning electron microscopy. II. Analysis of three estimators of surface roughness in second-dimension and third-dimension. *Microsc Microanal* 11, [redacted].

Buckley, M. & Yang, J. (1997). Regularised shortest-path extraction. *Patt Recogn Lett* 18 (7), 621–629.

Dong, W.P., Sullivan, P.J. & Stout, K.J. (1994). Comprehensive study of parameters for characterizing third-dimensional surface topography. III: Parameters for characterizing amplitude and some functional properties. *Wear* 178, 29–43.

Ladaga, J.L & Bonetto, R.B. (2002). Characterisation of texture in scanning electron microscope images. In *Advances in Imaging and Electron Physics*, Vol. 120, Hawkes, Peter W. (Ed.), pp. 136–189. San Diego, CA: Academic Press.

Lane, G.S. (1972). Dimensional measurements. In *The Use of the Scanning Electron Microscope*, Hearle, J.W.S., Sparrow, J.T. & Cross, P.M. (Eds.), pp. 219–238. New York: Pergamon Press.

Russ, J.C. (1994). *Fractal Surfaces*. New York, London: Plenum Press.

Sayles, R.S. & Thomas, T.R. (1978). Surface topography as a nonstationary random process. *Nature* 271, 431–434.

Stout, K.J., Sullivan, P.J., Dong, W.P., Mainsah, E., Luo, N., Mathia, T. & Zahouani, H. (1993). In *The Development of Methods for the Characterization of Roughness in 3 Dimensions.* Commission of the European Communities (BCR-3374/1/0/
1 170/90/2).

Sun, C. (1998). Multi-resolution rectangular subregioning stereo matching using fast correlation and dynamic programming techniques. CSIRO Mathematical and Information Sciences, Australia, Technical Report 98/246.

Sun, C. (2002). Fast stereo matching using rectangular subregioning and 3D maximum-surface techniques. *Inter J Comput Vision* 47 (1/2/3), 99–117.

Thomas, T.R., Rosén, B.G. & Amini, N. (1999). Fractal characterization of the anisotropy of rough surfaces. *Wear* 232, 41–50.